Two-pion interferometry in heavy ion collisions at HIRFL-CSR energy*

YU Li-Li(于莉莉)[1] JIRIMUTU(吉日木图)[1] ZHANG Wei-Ning(张卫宁)[1,2,3;1)]
HUO Lei(霍雷)[1] ZHANG Jing-Bo(张景波)[1]

1 (Department of Physics, Harbin Institute of Technology, Harbin 150006, China)
2 (School of Physics and Optoelectronic Technology, Dalian University of Technology, Dalian 116024, China)
3 (Center of Theoretical Nuclear Physics, National Laboratory of Heavy Ion Accelerator of Lanzhou, Lanzhou 730000, China)

Abstract We examine the two-pion Hanbury-Brown-Twiss (HBT) interferometry for the particle-emitting source produced in heavy ion collisions at HIRFL-CSR energy. The source evolution is described by relativistic hydrodynamics with three kinds of equations of state for chemical equilibrium (CE), chemical freeze-out (CFO), and partial chemical equilibrium (PCE) models, respectively. We investigate the effects of particle decay, multiple scattering, and source collective expansion on the two-pion interferometry results. We find that the HBT radii of the evolution source for the CFO and PCE models are smaller than that for the CE model. The HBT lifetime for the CFO model is smaller than those for the PCE and CE models. The particle decay increases the HBT radius and lifetime while the source expansion decreases the HBT radius. The multiple scattering effect on the HBT results can be neglected based on our model calculations.

Key words two-pion interferometry, HIRFL-CSR energy, particle decay, multiple scattering

PACS 25.75.-q, 25.75.Gz

1 Introduction

Two-pion interferometry (Hanbury-Brown-Twiss effect) has been extensively used in high energy heavy ion collisions to probe the space-time structure of the particle-emitting source[1—4]. The particle-emitting sources produced in high energy heavy ion collisions undergo an evolution from the initial state with high temperature and energy density to the chemical freeze-out where the observed particle ratios are fixed, and finally to the thermal freeze-out where the shapes of the particle momentum distributions are fixed[5]. The evolution of the source can be described by relativistic hydrodynamics, which has a great success in high energy heavy ion collisions[6, 7]. CSR (Cooling Storage Ring) is a new accelerator under commissioning at the Heavy Ion Research Facility in Lanzhou (HIRFL)[8]. The bombarding energy of HIRFL-CSR for heavy ion will reach around 1 AGeV. At this energy the collisions are full stopped, and a baryon density of 2—3 times normal nuclear matter density ($\rho_0 \sim 0.17$ fm^{-3}) is expected to be reached[9]. At HIRFL-CSR energy the particle-emitting source is a system of mixed hadronic gas with finite baryon density. There are "excited-state" particle decay and multiple scattering of particles in the source. These effects and the source collective expansion will influence the two-pion HBT results. In Refs. [10, 11] Wong studied the effects of source collective expansion and multiple scattering on two-pion HBT correlation function with a quantum probability amplitudes in a path-integral formalism. Using this quantum path-integral formulism of two-pion interferometry, Zhang et al. investigated the effect of multiple scattering on HBT radius for the sources produced at AGS energy based on the chemical equilibrium (CE) hydrodynamical model[12]. Recently, the effects of source collective expansion, multiple scattering, and excited-state decay on HBT radius are investigated for the sources produced at AGS and RHIC energies[13, 14]. In this paper we will examine the two-pion interferometry based on quantum

Received 14 February 2008
* Supported by National Natural Science Foundation of China (10575024, 10775024)
1) E-mail: weiningzh@hotmail.com

integral formulism for the particle-emitting sources produced at HIRFL-CSR energy. We will investigate the effects of particle decay, multiple scattering, and source expansion on HBT results of radius and lifetime.

2 Source evolution and equation of state

2.1 Relativistic hydrodynamic equations

In high energy heavy ion collisions, the dynamics of ideal fluid is defined by the local conservations of energy-momentum and net charges[6, 7]. The continuity equations of the conservations of energy-momentum, net baryon number, and entropy of the source are[6, 7]

$$\partial_\mu T^{\mu\nu}(x)=0\,, \tag{1}$$

$$\partial_\mu n_{\rm b}^{\mu}(x)=0\,, \tag{2}$$

$$\partial_\mu s^{\mu}(x)=0\,, \tag{3}$$

where x is the space-time coordinate of a thermalized fluid element in the center-of-mass frame of the source, $T^{\mu\nu}(x)$ is the energy-momentum tensor of the element, $n_{\rm b}^{\mu}(x)=n_{\rm b}(x)u^{\mu}$ and $s^{\mu}(x)=s(x)u^{\mu}$ are the four-current-density of baryon and entropy ($n_{\rm b}$ and s are the baryon density and entropy density), and $u^{\mu}=\gamma(1,\boldsymbol{v})$ is the 4-velocity of the element. The energy momentum tensor $T^{\mu\nu}(x)$ is given by[6, 7]

$$T^{\mu\nu}(x)=\big[\epsilon(x)+p(x)\big]u^{\mu}(x)u^{\nu}(x)-p(x)g^{\mu\nu}\,, \tag{4}$$

where p and ϵ are the pressure and energy density of the fluid element, and $g^{\mu\nu}$ is the metric tensor.

For simplicity we consider that the particle-emitting sources have spherical geometry. The local conservations Eqs. (1)—(3) give[6]

$$\partial_t E+\partial_r[(E+p)v]=-\frac{2v}{r}(E+p)\,, \tag{5}$$

$$\partial_t M+\partial_r(Mv+p)=-\frac{2v}{r}M\,, \tag{6}$$

$$\partial_t N_{\rm b}+\partial_r(N_{\rm b}v)=-\frac{2v}{r}N_{\rm b}\,, \tag{7}$$

$$\partial_t N_{\rm s}+\partial_r(N_{\rm s}v)=-\frac{2v}{r}N_{\rm s}\,, \tag{8}$$

where $E\equiv T^{00}$, $M\equiv T^{0r}$, $N_{\rm b}=n_b\gamma$, $N_{\rm s}=s\gamma$.

In our calculations, we assume that the system initially distributes in a sphere with radius r_0 uniformly and has zero velocity. With the initial conditions and after knowing equation of state, one can obtain the solutions of Eqs. (5)—(8)[6, 12—15] using the HLLE scheme[16, 17] and Sod's operator splitting method[18]. The grid spacing and time step in our calculations are taken as $\Delta x=0.02r_0$ and $\Delta t=0.99\Delta x$.

2.2 Equations of state

In order to obtain the solution of Eqs. (5)—(8) we need the equation of state $p(\epsilon,n_{\rm b},s)$, which gives the relationship of p, ϵ, $n_{\rm b}$, and s. In our calculations, we use a mixed perfect gas of hadrons to describe the particle-emitting source produced in the heavy ion collisions at HIRFL-CSR energy. The number density, energy density, pressure, and entropy density of the particle species i in the local frame of the element can be expressed in terms of the local temperature $T(x)$ and chemical potential $\mu_{\rm i}(x)$ as

$$n_{\rm i}=\frac{4\pi g_{\rm i}}{(2\pi)^3}\int_{m_{\rm i}}^{\infty}f_{\rm i}E\sqrt{E^2-m_{\rm i}^2}\,{\rm d}E\,, \tag{9}$$

$$\epsilon_{\rm i}=\frac{4\pi g_{\rm i}}{(2\pi)^3}\int_{m_{\rm i}}^{\infty}f_{\rm i}E^2\sqrt{E^2-m_{\rm i}^2}\,{\rm d}E\,, \tag{10}$$

$$p_{\rm i}=\frac{1}{3}\frac{4\pi g_{\rm i}}{(2\pi)^3}\int_{m_{\rm i}}^{\infty}f_{\rm i}(E^2-m_{\rm i}^2)^{3/2}\,{\rm d}E\,, \tag{11}$$

$$\begin{aligned}s_{\rm i}\;=\;&\frac{4\pi g_{\rm i}}{(2\pi)^3}\int_{m_{\rm i}}^{\infty}[-f_{\rm i}\ln f_{\rm i}\mp(1\mp f_{\rm i})\times\\&\ln(1\mp f_{\rm i})]E\sqrt{E^2-m_{\rm i}^2}\,{\rm d}E\,,\end{aligned} \tag{12}$$

where

$$f_{\rm i}=\frac{1}{\exp[(E-\mu_{\rm i})/T]\pm1}\,, \tag{13}$$

the sign (+) or (−) is for fermions or bosons, and $g_{\rm i}$ and $m_{\rm i}$ are the internal freedom and mass of particle species i. In the center-of-mass frame of the source, the fluid energy density ϵ, pressure p, and entropy density s are the sum of $\epsilon_{\rm i}$, $p_{\rm i}$, and $s_{\rm i}$ over all particle species in the mixed hadronic gas. The baryon density $n_{\rm b}$ is the sum of $n_{\rm i}$ for all the baryon species in the mixed hadronic gas. In our model calculations we only consider N, π, K, and Δ(1232) in the sources for simplicity.

2.2.1 Chemical equilibrium

For the chemical equilibrium (CE) model, there are always chemical reaction equilibrium in the source before it breakup at the thermal freeze-out characterized by the temperature $T^{\rm th}$. So the chemical freeze-out and the thermal freeze-out are coincident in this model. We assume that all observed particles are produced thermally from the source configuration at $T^{\rm th}$. The chemical potentials of the particles satisfy

$$\mu_{\rm N}=\mu_{\Delta}=\mu_{\rm b}, \tag{14}$$

$$\mu_{\pi}=\mu_{\rm K}=0, \tag{15}$$

where $\mu_{\rm b}$ is the baryon chemical potential which is constant in the CE model.

2.2.2 Chemical freeze-out

In opposition to the CE model, the chemical freeze-out (CFO) model assumes that there are not any chemical reactions after the chemical freeze-out characterized by the temperature $T^{\rm ch} > T^{\rm th}$. Below $T^{\rm ch}$, all numbers of the hadrons in the source are fixed, that is $\partial_\mu(n_{\rm i}u^\mu) = 0$. Because of entropy conservation, $\partial_\mu(s\,u^\mu) = 0$, one can assume that below $T^{\rm ch}$ the ratio of $n_{\rm i}$ to s obeys[5]

$$\frac{n_{\rm i}(T,\mu_{\rm i})}{s(T,\{\mu_{\rm i}\})} = \frac{n_{\rm i}(T^{\rm ch},\mu_{\rm i}^{\rm ch})}{s(T^{\rm ch},\{\mu_{\rm i}^{\rm ch}\})}\,. \tag{16}$$

From this equation we can obtain the chemical potential $\mu_{\rm i}(T)$ as a function of temperature after the chemical freeze-out, which ensures keeping the number of the hadron i fixed.

2.2.3 Partial chemical equilibrium

Because the final particles are composed of the contributions from direct particle productions and excited-state particle decays, a partial chemical equilibrium (PCE) model, in which some processes with larger cross sections can be equilibrated even below $T^{\rm ch}$, is a more realistic case[5, 19]. For the PCE model Eq. (16) is replaced by[5, 19]

$$\frac{\bar{n}_{\rm i}(T,\mu_{\rm i})}{s(T,\{\mu_{\rm i}\})} = \frac{\bar{n}_{\rm i}(T^{\rm ch},\mu_{\rm i}^{\rm ch})}{s(T^{\rm ch},\{\mu_{\rm i}^{\rm ch}\})}\,, \tag{17}$$

where $\bar{n}_{\rm i} = n_{\rm i} + \sum_{\rm j\neq i}\tilde{d}_{\rm j\to i}\,n_{\rm j}$, $\tilde{d}_{\rm j\to i}$ is the fraction of that the excited-state particle species j decays to the stable particle species i[5, 19]. In our model calculations we consider N, π, and K as stable particles, and Δ(1232) as excited-state particle.

Figure 1 shows the chemical potential $\mu_{\rm i}(T)$ as a function of T for the sources produced in the heavy ion collisions at HFRIL-CSR energy. In the calculations, the chemical freeze-out temperature and thermal freeze-out temperature are taken as 76 and 40 MeV. The chemical potentials for CFO are calculated with Eq. (16). The chemical potentials of the stable particles for PCE are calculated with Eq. (17), and the chemical potentials of the excited-state particles for PCE are obtained from the relation of chemical equilibrium, $\mu_\Delta = \mu_{\rm N} + \mu_\pi$. After knowing the chemical potentials of the hadrons in the source, one can obtain the EOS, $p\,(\epsilon, n_{\rm b}, s)$, from Eqs. (9)—(12), and then obtain the solution of motion Eqs. (5) — (8) with initial conditions[6, 12—15].

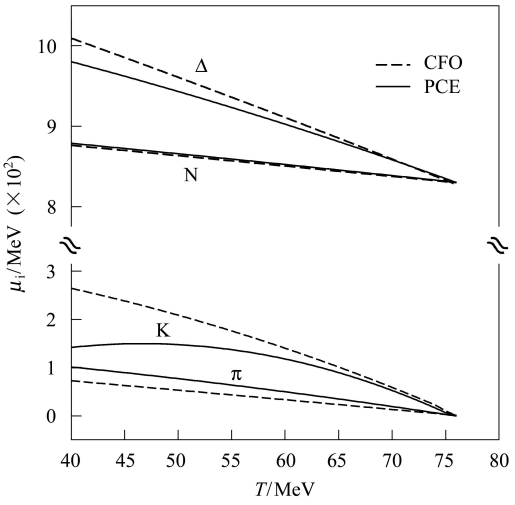

Fig. 1. Chemical potentials of hadrons for CFO (dashed lines) and PCE (solid lines) in heavy ion collisions at HIRFL-CSR energy.

2.3 Source evolution

In the calculations of the two-pion correlation functions for the evolutional sources we need the source temperature and expanding velocity, which can be obtained from the solution of the equations of motion (5)—(8). Fig. 2(a) and (b) show the isotherms and velocity profiles for the evolutional source. The initial temperature and baryon chemical potential in our calculations are taken as T_0 = 100 MeV and $\mu_{\rm b0}$ = 810 MeV, which correspond to an initial energy density of $\epsilon_0 = 0.47$ GeV/fm^3 and a baryon density of $n_{\rm b0} = 0.42$ fm^{-3}. The chemical freeze-out temperature is taken as $T^{\rm ch} = 76$ MeV, and the corresponding chemical potential is 830 MeV. They are consistent with the extrapolations obtained from hadronic abundances at CERN/SPS, NBL/AGS, GSI/SIS[20, 21]. Based on the criteria of the dependance of thermal freeze-out temperature to the system energy density[22], the thermal freeze-out temperature is chosen as $T^{\rm th}$ = 40 MeV, which corresponds to a thermal freeze-out energy density ϵ = 47 MeV/fm^3

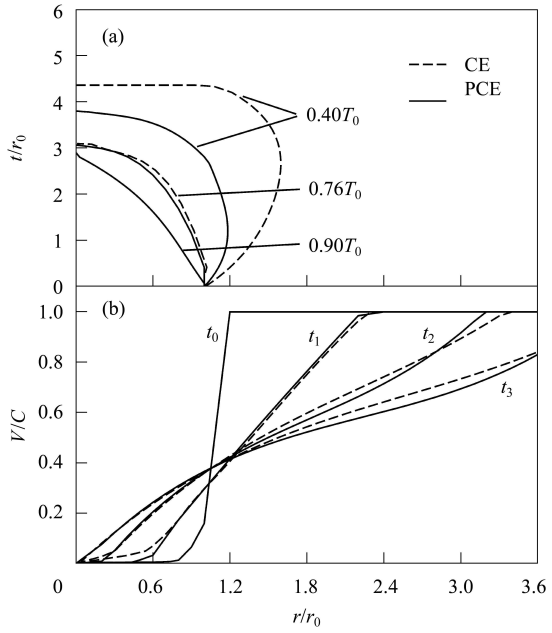

Fig. 2. (a) Isotherms and (b) velocity profiles of the evolutional source.

close 45 MeV/fm^3 predicted in Ref. [22]. From Fig. 2(a) and (b), it can be seen that the space-time geometry at $T^{\rm th}$ for the PCE model is much smaller than that for the CE model, and the source expanding velocities for the two models are somewhat different. Our calculations indicate that the isotherm and velocity results for the CFO model are close to those for the PCE model.

3 HBT analysis

3.1 Two-pion interferometry formulas

The two-pion HBT correlation function is defined as the ratio of the two identical pion (for example π^+) momentum distribution $P(k_1,k_2)$ to the product of single-pion momentum distribution $P(k_1)P(k_2)$. For an evolutional source, using quantum probability amplitudes in a path-integral formalism, $P(k_{\rm i})$ $(i=1,2)$ and $P(k_1,k_2)$ can be expressed as[10]:

$$P(k)=\int {\rm d}^4x\,{\rm e}^{-2\,\mathcal{I}{\rm m}\,\bar{\phi}_s(x)}\rho(x)A^2(\kappa(x),x)\,, \qquad (18)$$

$$P(k_1,k_2)=\int {\rm d}^4x_1{\rm d}^4x_2\,{\rm e}^{-2\,\mathcal{I}{\rm m}\,\bar{\phi}_s(x_1)}{\rm e}^{-2\,\mathcal{I}{\rm m}\,\bar{\phi}_s(x_2)}\times \rho(x_1)\rho(x_2)|\Phi(\kappa_1\kappa_2:x_1x_2\to x_{d1}x_{d2})|^2, \qquad (19)$$

where $A(\kappa(x),x)$ is the magnitude of the amplitude for producing a pion with momentum κ at x; $\rho(x)$ is the four-dimension density of the identical pion source. ${\rm e}^{-2\,\mathcal{I}{\rm m}\,\bar{\phi}_s(x)}$ is the absorption factor due to multiple scattering[10—12], and $\Phi(\kappa_1\kappa_2:x_1x_2\to x_{d1}x_{d2})$ is the wave function for the two pions produced at x_1 and x_2 with momenta κ_1 and κ_2, and detected at x_{d1} or x_{d2} with momenta k_1 and k_2, respectively,

$$\Phi(\kappa_1\kappa_2:x_1x_2\to x_{d1}x_{d2})= \frac{1}{\sqrt{2}}\Big\{\bar{A}(\kappa_1x_1\to k_1x_{d1})\bar{A}(\kappa_2x_2\to k_2x_{d2})\times {\rm e}^{-{\rm i}k_1\cdot(x_{d1}-x_1)-{\rm i}k_2\cdot(x_{d2}-x_2)}+(x_1\leftrightarrow x_2)\Big\}, \qquad (20)$$

where $(x_1\leftrightarrow x_2)$ represents the symmetric term to the former by exchanging x_1 and x_2,

$$\bar{A}(\kappa x\to kx_d)=A(\kappa x)\,{\rm e}^{{\rm i}\delta_{mf}(\kappa x\to kx_d;x')}\,, \qquad (21)$$

$\delta_{mf}(\kappa x\to kx_d;x')$ is the phase shift associated with the source collective motion[10, 11],

$$\delta_{mf}(\kappa x\to kx_d;x')=-\int_x^{x_{\rm f}}[\ \kappa(x')-k\ ]\cdot{\rm d}x'\ . \qquad (22)$$

Based on Glauber multiple scattering theory[23], the absorption factor due to multiple scattering can be written as[10—12]

$${\rm e}^{-2\,\mathcal{I}{\rm m}\,\bar{\phi}_s(x)}=\exp\left[-\int_x^{x_{\rm f}}\Big(\sum\nolimits_{\rm i}{}'\sigma_{\rm abs}({\pi}{\rm i})\,n_{\rm i}(x)\Big){\rm d}\ell\right], \qquad (23)$$

where $\sum'_{\rm i}$ means the summation for the medium particles along the propagating path element, ${\rm d}\ell$, of the considered pion, $\sigma_{\rm abs}({\pi}{\rm i})$ is the absorption cross section of the pion with the medium particle i, and the integral is carried out from the production point x of the pion to the thermal freeze-out point $x_{\rm f}$.

From Eqs. (18), (19), and (23), one can see that in the two-pion interferometry the multiple scattering modifies the pion source density $\rho(x)$ by the absorption factor, which is related to the cross section $\sigma_{\rm abs}({\pi}{\rm i})$. For the sources produced at HIRFL-CSR energy, the dominant absorption processes are $\pi^+{\rm N}\to\Delta$ and $\pi^+\pi^-\to\pi^0\pi^0$. We calculate the cross-section for $\pi^+{\rm N}\to\Delta$ by

$$\sigma_{\rm abs}(\pi^+{\rm N}\to\Delta)=\frac{2}{3}\frac{\sigma_0\,(\Gamma_\Delta/2)^2}{(\sqrt{s_{\pi{\rm N}}}-m_\Delta)^2+(\Gamma_\Delta/2)^2}\,, \qquad (24)$$

where $\Gamma_\Delta=120$ MeV, $m_\Delta=1232$ MeV, and $\sigma_0=200$ mb. The cross-section for $\pi^+\pi^-\to\pi^0\pi^0$ can be expressed as[24, 25]:

$$\sigma_{\rm abs}(\pi^+\pi^-\to\pi^0\pi^0)=\frac{8}{9}\frac{\pi}{p_{\rm cm}^2}\sin^2(\delta_0-\delta_2)\,, \qquad (25)$$

where $p_{\rm cm}=\sqrt{s_{\pi\pi}-4m_\pi^2}/2$ and the phase shifts δ_0 and δ_2 are given by Ref. [25].

In the CFO and CE models the identical pions are produced thermally at $T^{\rm ch}$ and $T^{\rm th}$, respectively. However, in the PCE model the identical pions contain the direct-produced pions produced at $T^{\rm ch}$ as well as the decayed pions produced between $T^{\rm ch}$ and $T^{\rm th}$. The four-dimension density of the pion source in the PCE model is

$$\rho(x)=n_\pi(x)\delta(t'-\tau^{\rm ch})+\sum_{{\rm j}\neq\pi}D_{{\rm j}\to\pi}n_{\rm j}(x)\,, \qquad (26)$$

where $\tau^{\rm ch}$ is the freeze-out time in local frame and $D_{{\rm j}\to\pi}$ is the product of the decay rate in time and the fraction of the decay $\tilde{d}_{{\rm j}\to\pi}$. For example, $D_{\Delta\to\pi}=\Gamma_\Delta\times\dfrac{1}{3}$ and $D_{\pi^0\pi^0\to\pi^+\pi^-}=v_r n_\pi\sigma(\pi^0\pi^0\to\pi^+\pi^-)\times1$, where v_r is the relative velocity of the two colliding pions and $\sigma(\pi^0\pi^0\to\pi^+\pi^-)$ equals the absorption cross section $\sigma_{\rm abs}(\pi^+\pi^-\to\pi^0\pi^0)$ in Eq. (25).

3.2 Two-pion interferometry results

Using the formulas of two-pion interferometry discussed in the last subsection we can calculate the two-pion and single-pion momentum distributions, $P(k_1,k_2)$ and $P(k)$, by Monte Carlo method[12—14, 26]. Taking the relative momentum and energy of the two pions, $q=|\boldsymbol{k}_1-\boldsymbol{k}_2|$, $q_0=|k_{01}-k_{02}|$, as variables, we can construct the two-pion HBT correlation function

$C(q,q_0)$ from $P(k_1,k_2)$ and $P(k_1)P(k_2)$ by integrating over $\boldsymbol{k}_1$, $\boldsymbol{k}_2$ for each (q, q_0) bin[12—14, 26].

Figure 3(a) shows the two-pion correlation functions $C(q, q_0 < 15$ MeV) for the evolutional sources with the three kinds of equations of state, CFO, PCE, and CE. In order to compare their HBT results, we take the same initial radius, $r_0 = 6$ fm, and the same initial temperature and chemical potential as discussed in subsection 2.3 in our calculations for the three models. The same initial conditions correspond to the same impact parameter in experimental data analysis. In order to investigate the effect of the source expansion on the HBT results, we also examine the two-pion interferometry for the corresponding "static sources", which have the same space-time configuration with the evolutional sources but the expanding velocities of the pion-emitting sources are forced to be zero[13]. Fig. 3(b) shows the two-pion HBT correlation functions for the "static sources". In Fig. 3 the curves are the fitted results with the parameterized formula of Gaussian source distribution

$$C(q,q_0) = 1 + \lambda \mathrm{e}^{-q^2R^2 - q_0^2\tau^2} \ . \tag{27}$$

Table 1 gives the fitted results of the HBT radius R, lifetime τ, and the chaotic parameter λ of the sources. As we discussed in the last subsection, the effect of the multiple scattering (MS) on the two-pion interferometry can be expressed as the absorption factor $\mathrm{e}^{-2\mathcal{I}\mathrm{m}\,\bar{\phi}_s(x)}$. In order to investigate this effect on the HBT results, we also calculate the two-pion correlation functions without the absorption factor for the PCE model. These results are listed in Table 1 labeled with "without MS abs.".

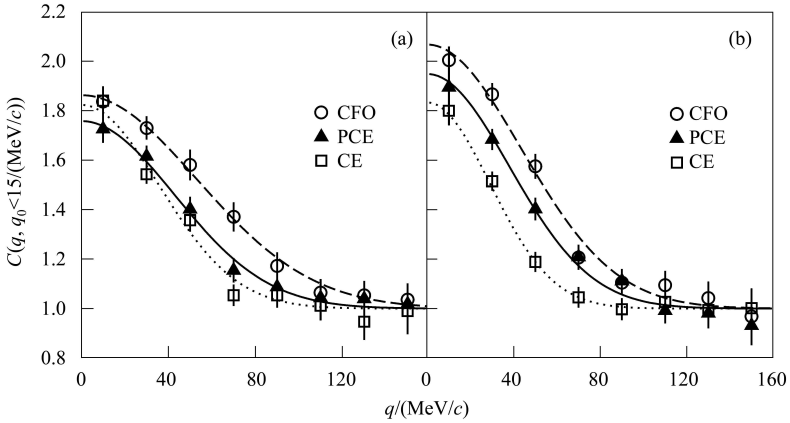

Fig. 3. The two-pion HBT correlation functions for the (a) evolutional sources and (b) the corresponding "static sources".

Table 1. The HBT fitted results.

	CFO	PCE		CE
		with MS abs.	without MS abs.	
(a)	$R = 2.86 \pm 0.13$ fm	$R = 3.30 \pm 0.18$ fm	$R = 3.25 \pm 0.18$ fm	$R = 3.91 \pm 0.22$ fm
evolutional	$\tau = 6.35 \pm 0.32$ fm	$\tau = 7.48 \pm 0.44$ fm	$\tau = 7.61 \pm 0.46$ fm	$\tau = 7.40 \pm 0.47$ fm
source	$\lambda = 0.95 \pm 0.04$	$\lambda = 0.91 \pm 0.05$	$\lambda = 0.84 \pm 0.05$	$\lambda = 0.91 \pm 0.05$
(b)	$R = 3.22 \pm 0.12$ fm	$R = 3.50 \pm 0.15$ fm	$R = 3.68 \pm 0.17$ fm	$R = 4.81 \pm 0.29$ fm
"static	$\tau = 5.01 \pm 0.28$ fm	$\tau = 6.63 \pm 0.34$ fm	$\tau = 7.30 \pm 0.39$ fm	$\tau = 9.44 \pm 0.87$ fm
source"	$\lambda = 1.12 \pm 0.04$	$\lambda = 1.09 \pm 0.05$	$\lambda = 1.05 \pm 0.05$	$\lambda = 0.98 \pm 0.07$

From the HBT results we can see that the HBT radii for the CFO and PCE models are smaller than those for the CE model, because in the CE model the source has large space geometry at T^{th} (see Fig. 2(a)). The excited-state particle decays between the chemical freeze-out and the thermal freeze-out lead to the HBT radii and lifetimes for the PCE model larger than those for the CFO model. In the PCE model the pions subject to the multiple scattering of the particles in the source. However, our calculations indicate that the effect of multiple scattering on the HBT results is small and can be neglected for the heavy ion collisions at HIRLF-CSR energy. By comparing the results for the evolutional sources and the corresponding "static sources", we can see that the effect of the source expansion decreases the HBT radii[13, 27]. After removing the effect of the source expansion, the "static source" HBT results of radius and lifetime for the CFO, PCE, and CE models are consistent with the space-time geometry of the sources (see Fig. 2(a)).

The results of the chaotic parameter λ for the "static sources" for the CFO and PCE models are larger than those for the evolutional sources. The values of λ differ from unit because the space-time distributions of the pion sources are not Gaussian exactly.

4 Summary and conclusions

We examine the two-pion interferometry in the heavy ion collisions at HIRFL-CSR energy. The particle-emitting sources are described by relativistic hydrodynamics with three kinds of equations of state for the CE, CFO, and PCE models, respectively. In the CE model the evolution of the source is chemical equilibrated until the thermal freeze-out, so all final particles are produced at the thermal freeze-out configuration. In the CFO model, the final particles are produced at the chemical freeze-out configuration and move with the source until the thermal freeze-out. A more realistic model is the PCE model. In this model the final particles include the direct CFO produced particles and the decayed particles produced during the source evolving from the chemical freeze-out to the thermal freeze-out. We calculate the HBT correlation functions using the quantum path-integral formulism of two-pion interferometry and investigate the effects of multiple scattering, the excited-state particle decay, and the source expansion on the two-pion interferometry results. Our HBT analysis results indicate that under the same source initial conditions the HBT radii for the CFO and PCE models are smaller than those for the CE model. The excited-state particle decays lead to the HBT radii and lifetimes for the PCE model larger than those for the CFO model. The effect of multiple scattering on the HBT results is small and can be neglected for the heavy ion collisions at HIRLF-CSR energy. In addition, we find that the effect of the source expansion decreases the HBT radii and the "static source" HBT results of radius and lifetime for the CFO, PCE, and CE models are consistent with the space-time geometry of the sources.

We thank Cheuk-Yin Wong for helpful discussions.

References

1 Wong C Y. Introduction to High-Energy Heavy-Ion Collisions. Singapore: World Scientific, 1994.
2 Wiedemann U A, Heinz U. Phys. Rept., 1999, **319**: 145
3 Weiner R M. Phys. Rept., 2000, **327**: 249
4 Lisa M, Pratt S, Soltz R, Wiedemann U. Ann. Rev. Nucl. Prat. Sci., 2005, **55**: 357; nucl-ex/0505014
5 Hirano T, Tsuda K. Phys. Rev. C, 2002, **66**: 054905
6 Rischke D H, Gyulassy M. Nucl. Phys. A, 1996, **680**: 479; Rischke D H. nucl-th/9809044
7 Kolb P, Heinz U. nucl-th/0305084
8 ZHENG C, XIAO Z G, XU H S et al. HEP & NP, 2007, **31**(12): 1177 (in Chinese)
9 Wagner A, Muntz C, Oeschler H et al. Phys. Lett. B, 1997, **420**: 20
10 Wong C Y. J. Phys. G, 2003, **29**: 2151; Wong C Y. J. Phys. G, 2004, **30**: S1053
11 Wong C Y. AIP Conference Proc., 2006, **828**: 617; hep-ph/0510258
12 ZHANG W N, Efaaf M J, Wong C Y, Khaliliasr M. Chin. Phys. Lett., 2004, **21**: 1918
13 Efaaf M J, ZHANG W N, Khaliliasr et al. HEP & NP, 2005, **29**(1): 46; Efaaf M J, ZHANG W N, Khaliliasr et al. HEP & NP, 2005, **29**(5): 467 (in Chinese)
14 YU L L, ZHANG W N, Wong C Y. Phys. Rev. C, 2008, **78**: 014908
15 ZHANG W N, Efaaf M J, Wong C Y. Phys. Rev. C, 2004, **70**: 024903
16 Schneider V et al. J. Comput. Phys., 1993, **105**: 92
17 Rischke D H, Bernard S, Maruhn J A. Nucl. Phys. A, 1995, **595**: 346
18 Sod G A. J. Fluid Mech., 1977, **83**: 785
19 Bebie H, Gerber P, Goity J L, Leutwyer H. Nucl. Phys. B, 1992, **378**: 95
20 Cleymans J, Redlich K. Phys. Rev. Lett., 1998, **81**: 5284
21 XIAO Z G. talk presented at QM2006, Shanghai, China, 14—20 NoV 2006
22 Cleymans J, Redlich K. Phys. Rev. C, 1999, **60**: 054908
23 Glauber R J. Lectures in Theoretical Physics. Interscience, N.Y., 1959. 315
24 Martin B R, Morgan D, Shaw G. Pion-Pion Interaction in Particle Physics. Academic Press, 1976. 101
25 Yndurain F J. hep-ph/0212282
26 ZHANG W N, LIU Y M, WANG S et al. Phys. Rev. C, 1993, **47**: 795; ZHANG W N, LIU Y M, HUO L et al. Phys. Rev. C, 1995, **51**: 922; ZHANG W N, HUO L CHEN X J et al. Phys. Rev. C, 1998, **58**: 2311; ZHANG W N, LI S X, Wong C Y, Efaaf M J. Phys. Rev. C, 2005, **71**: 064908
27 Pratt S. Phys. Rev. Lett., 1984 **53**: 1219